# Transverse momenta of hadronically produced heavy-quark systems: $2 \to 3$ processes in quantum chromodynamics

Z. Kunszt,* E. Pietarinen, and E. Reya
*Deutsches Elektronen-Synchrotron DESY, Hamburg, West Germany*
(Received 1 June 1979)

Transverse-momentum spectra are calculated for heavy quarkonium states $Q\bar{Q}$ ($J/\psi$,$\Upsilon$) produced in $pp$ and $\bar{p}p$ collisions. These transverse momenta result from the hard quark ($q$) and gluon ($g$) subprocesses $q\bar{q} \to Q\bar{Q}g$, $gq \to Q\bar{Q}q$, and $gg \to Q\bar{Q}g$. The $p_T$ distributions for $J/\psi$ production are expected to be significantly steeper than for the $\mu^+\mu^-$ continuum, whereas the two distributions become similar in the $\Upsilon$ mass region. These effects are partly confirmed by recent CERN ISR measurements. Predictions for $\bar{p}p$ collisions at $\sqrt{s} = 540$ GeV are also given.

Recent measurements[1] of the dimuon spectrum near the $\Upsilon$ region in proton-nucleus scattering at $\sqrt{s} = 27.4$ GeV have revealed that the mean transverse momentum of the $\Upsilon$ is significantly higher than the corresponding value for the (Drell-Yan) dimuon continuum, the latter being independent of the dimuon mass $M$ above 5 GeV. Typically, $\langle p_T \rangle_\Upsilon$ is about 20% larger than the continuum value $\langle p_T \rangle_{\mu^+\mu^-}$. Similar effects have been found in the $J/\psi$ region[2,3] and, although inferior in statistics, ISR measurements[4] might also be consistent with this observed trend of the $p_T$ spectrum off and on resonance. *A priori*, possible differences in the $p_T$ distributions on and off resonance are not unexpected since in quantum chromodynamics (QCD) the production mechanisms for heavy quarkonium ($Q\bar{Q}$) states and continuum dimuons are fundamentally different. Whereas the lowest-order subprocesses for producing a muon pair at $p_T \neq 0$ are $q\bar{q} \to \mu^+\mu^- g$ and $gq \to \mu^+\mu^- q$, the leading contribution to the transverse momentum of a given quarkonium state comes from the purely hadronic $2 \to 3$ processes $q\bar{q} \to Q\bar{Q}g$, $gq \to Q\bar{Q}q$, and $gg \to Q\bar{Q}g$, where the light and heavy quarks are denoted by $q = u, d, s$ and $Q = c, b, \ldots$, respectively, and $g$ stands for the gluon. Because of the complexity of calculating $2 \to 3$ subprocesses (keeping $m_Q \neq 0$), no serious attempt has been made so far to investigate the effects of hard-gluon bremsstrahlung for the $p_T$ spectra of quarkonium states (charmonium etc.) as compared to the one of the familiar Drell-Yan dimuons. It is the purpose of this article to discuss and calculate these typical QCD effects and to compare them with recent measurements of hadronically produced heavy quarkonium states.

Before discussing the more involved case of transverse momenta of quarkonium states let us briefly recapitulate the situation of the familiar Drell-Yan process. To order $\alpha_s$ the transverse momenta of massive lepton pairs are due to the two subprocesses[5-8] shown in Fig. 1. The cross section for dimuon production from initial hadrons $A$ and $B$ is obtained by convoluting the expressions for these subprocesses with the relevant parton distributions

$$\frac{d^2\sigma^{AB}}{dM\,dp_T^2} = \int dx_a\,dx_b\,f_a^A(x_a, q^2)\,f_b^B(x_b, q^2)\,\frac{d^2\sigma^{ab}}{dM\,dp_T^2}\,, \tag{1}$$

where all color factors are included in $d\sigma^{ab}$, which denotes the subprocess ($q\bar{q} \to \mu^+\mu^- g$ and $gq \to \mu^+\mu^- q$) cross section[6,7,9] for producing a dimuon pair with mass $M \equiv (q^2)^{1/2}$ and transverse momentum $p_T$ from partons $a$ and $b$. The predicted $p_T$ distributions at c.m. rapidity $y = 0$ differ only insignificantly from the $y$-averaged ones as given in Eq. (1). For our calculations we shall employ throughout the fully renormalization-group-improved QCD "counting-rule-like" quark and gluon distributions $f_a^A(x_a, q^2)$ of Ref. 10. Since the subprocess cross sections $d\sigma^{ab}/dp_T^2$ in Eq. (1) diverge as $p_T \to 0$ (i.e., parallel emission), there is some controversy as to what theoretical quantity should be confronted with experiment. Comparing directly the predictions of Eq. (1) with experiment, one finds[7,9] a reasonable agreement with the shape of the measured $p_T$ distribution for $p_T \geq 1$ GeV. On the other hand, comparing average dimuon transverse momenta[6,11] with experiment, i.e., $p_T$ moments $\langle p_T \rangle$ and $\langle p_T^2 \rangle$ as calculated from Eq. (1), which weigh the small-$p_T$ region of $d\sigma/dp_T^2$, yields contradicting results as to the size and importance of the in-

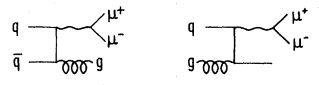


FIG. 1. Lowest-order contributions to transverse dimuon momenta (crossed diagrams are not shown).

trinsic transverse momenta $k_T$ of the initial quarks and gluons in Eq. (1) which, so far, are not predictable dynamically by QCD. Values for $\langle k_T \rangle$ between[11] 200 MeV and[6] 800 MeV have been suggested. Although only $p_T$ moments are well behaved[5] (finite) and therefore the prescription for calculating $\int p_T{}^n (d\sigma^{ab}/dp_T{}^2) dp_T{}^2$ for $n \geq 1$ is unambiguous, the integration down to small $p_T$ is delicate; $\alpha_s$ becomes substantially different and so may the scale breaking effects in the parton distributions $f_a^A$.

Since $d^2\sigma^{ab}/dM dp_T{}^2$ will contain terms such as $\log(M^2/p_T{}^2)$, the naive "hard scattering" perturbation theory in Eq. (1) breaks down for $p_T \ll M$ and one must sum[12] these logarithms to all orders in $\alpha_s$. Going beyond this double logarithmic approximation,[12] Parisi and Petronzio[13] have recently resummed even these double logarithms for the $q\bar{q}$ process and thus were able to compute the whole $p_T$ distribution, including $p_T \simeq 0$, from first principles for very large values of the c.m. energy $s$. These asymptotic predictions, however, do not adequately describe the data at moderate, i.e., currently available energies. The remaining discrepancy between these asymptotic predictions for the $p_T$ distribution and present measurements can then be removed by smearing these predictions in the small-$p_T$ region using some *ad hoc* ansatz for the smearing function[13]; this implies a somewhat reduced value for the average intrinsic transverse momentum of partons of about $\langle k_T \rangle \simeq 500$ MeV. Since, in the present context, we are mainly interested in the *difference* between the shape (slope) of the $p_T$ spectrum of dimuons and quarkonium states, which is little influenced by the (common) size of intrinsic transverse momenta, we shall only concentrate on the explicit $p_T$ distribution $d\sigma/dp_T{}^2$ for $p_T \gtrsim 1$ GeV, thus avoiding any complications due to soft (collinear) gluon emission.

Within the framework of QCD, the production of heavy-quark flavors in hadronic collisions is assumed to proceed via the fundamental subprocesses[14-18] $q\bar{q} \to Q\bar{Q}$ and $gg \to Q\bar{Q}$. In this way one can predict[18,19] even absolute cross sections for $J/\psi$, $\psi'$, $\Upsilon$, $\Upsilon'$, ... production in fair agreement with experiment. Apart from these lowest-order $\alpha_s{}^2$ contributions to the total production cross section, the transverse momenta of bound-heavy-quark states $Q\bar{Q}$ originate from hard-gluon radiation off the initial and final quark states as well as off the intermediate gluon, and are thus at least of order $\alpha_s{}^3$, namely, $q\bar{q} \to Q\bar{Q}g$, $gq \to Q\bar{Q}g$, and $gg \to Q\bar{Q}g$ as shown in Fig. 2. The $p_T$ distribution of the $Q\bar{Q}$ system is then formally given by a similar expression as in Eq. (1) but integrated over the invariant energy $M \equiv (q^2)^{1/2}$ of the $Q\bar{Q}$ system,

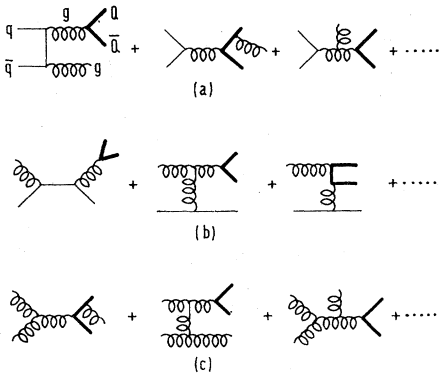


FIG. 2. Lowest-order contributions to the transverse momenta of heavy quarkonium states $Q\bar{Q}$. There are 5 diagrams for each process in (a) and (b), whereas the subprocess in (c) consists of 16 $ggg Q\bar{Q}$ Feynman diagrams and 5 ghost diagrams.

$$\frac{d\sigma^{ab}}{dp_T{}^2} = \int_{2m_Q}^{2m_0} dM \frac{d^2\sigma^{AB}}{dM dp_T{}^2}, \tag{2}$$

where for the coupling of the fundamental subprocesses we always take $\alpha_s = 12\pi/23 \ln(M^2/\Lambda^2)$ with $\Lambda \simeq 0.5$ GeV. Within the semilocal-duality approach[15-17,19] the upper limit of integration $2m_0$ should correspond to the threshold for open flavor $Q$ production ($D\bar{D}$, etc.), i.e., $2m_0 = 2m_D$ for charmonium and $2m_0 \simeq 10.4$ GeV for $b\bar{b}$ quarkonium. Furthermore, to obtain the absolute cross section for producing a definite $Q\bar{Q}$ bound state, the partonic cross sections in Eq. (2) should be divided[19] by the number of bound $Q\bar{Q}$ levels in the invariant-$Q\bar{Q}$-mass interval $M$ considered. Alternatively, one might also use $2m_0 = \sqrt{s}$ and/or employ only color-singlet projections[14,18] of the gluonic amplitudes, i.e., the quarkonium ground states are supposed to be dominantly produced via $p$-wave resonances. Since, in the present context, we are not interested in these detailed model assumptions, we shall state all our results with the normalization corresponding to Eq. (2); of course, if one wants to compare these results with measured *absolute* cross sections, they have to be multiplied by the appropriate duality (bound-state) division factors and by appropriate branching ratios. However, such ambiguities as well as the specific choice of $\alpha_s$ and of the heavy-quark mass $m_Q$, and the detailed structure of parton distributions affect mainly the absolute normalization of the cross section, but are of little influence as far as the shapes (slopes) of the $p_T$ distributions $d\sigma/dp_T{}^2$ are concerned. The important point of our investigation is to study the $p_T$ distribution in Eq. (2) on resonance *relative* to the one of the continuum dimuons in Eq. (1). This possible *difference* be-

tween the dimuon and the $Q\bar{Q}$ $p_T$ spectrum should be entirely due to dynamical QCD effects and is also independent of intrinsic parton $k_T$'s. On the other hand, at the present state of the art, we cannot calculate "uniquely" the $p_T$ moments directly since their definition involves total cross sections. This is because order $\alpha_s^3$ contributions to the leading-order $\alpha_s^2$ total cross section come not only from the diagrams of Fig. 2 but also from the so far unknown virtual gluon-loop corrections to the leading $q\bar{q} \to Q\bar{Q}$ and $gg \to Q\bar{Q}$ subprocesses. However, it should be emphasized that the cleanest test of effects due to hard-gluon radiation would be to compare *directly* the $p_T$ distribution for $p_T \geq 1$ GeV, and not just averaged quantities.

A detailed discussion of the calculation of the massless $2 \to 3$ scattering processes in QCD has been given in Ref. 20, where also a comparison of their relative magnitudes as well as their importance relative to the $2 \to 2$ subprocess can be found. The invariant matrix elements have been calculated using the algebraic computer program[21] REDUCE. The complexity of the calculation increases with the number of gluon lines since, unlike in QED, only physical transverse helicities have to be kept in the gluon polarization sum or instead one has to use a covariant (Feynman) gauge and add the contributions of ghost diagrams. Using this latter procedure, there are 5 Feynman diagrams for each process of Figs. 2(a) and 2(b), whereas the $gg \to Q\bar{Q}g$ subprocess in Fig. 2(c) consists of 16 $gggQ\bar{Q}$ Feynman diagrams and 5 ghost diagrams; thus we had to calculate 25 Cutkosky diagrams each for Figs. 2(a) and 2(b), and 281 Cutkosky diagrams for Fig. 2(c). The heavy-quark masses $m_Q$ for the diagrams in Fig. 2 have been taken to be $m_c = 1.25$ GeV and $m_b = 4.5$ GeV. In order to avoid infrared singularities, the differential cross sections have been calculated with a cut in the transverse momentum of the produced heavy quark, $p_T \geq 1$ GeV. We have checked our algebraic calculations by an entirely independent numerical procedure using helicity projectors. For further details and explicit analytic expressions of the fundamental cross sections we refer the interested reader to the Appendix.

In Figs. 3 and 4 we show our predictions for $d\sigma/dp_T^2$ at $\sqrt{s} = 27.4$ GeV and 63 GeV together with the existing data of Ref. 22 and Refs. 4 and 23, respectively. For comparison we also show $d^2\sigma/dMdp_T^2$ of the continuum in the appropriate dimuon mass region according to the graphs of Fig. 1. Again it should be emphasized that, as already discussed, only the $p_T$ shapes can be safely calculated for $p_T \geq 1$ GeV, whereas the absolute normalizations suffer from uncertainties such as the $q^2$-dependent gluon wave functions, the choice of $\alpha_s$, and from the details of the duality model assumptions for Eq. (2). As a general rule, the contributions to the $p_T$ spectrum from the $q\bar{q}$ and $gg$ subprocesses are always steeper than the contribution of $gq$ scattering. Therefore, at *small* values of $\sqrt{\tau} \equiv M/\sqrt{s}$ where the $gg$ subprocess gives a sizable contribution, we expect a different (stee-

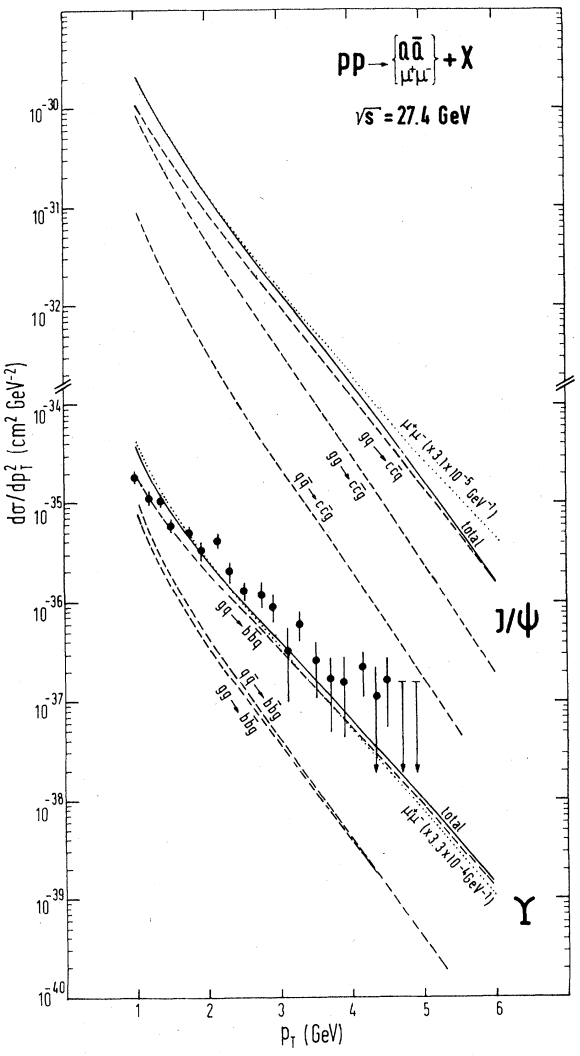


FIG. 3. QCD predictions (solid curves) for the $p_T$ distributions of $J/\psi$ and $\Upsilon$ production at $\sqrt{s} = 27.4$ GeV according to the diagrams in Fig. 2. The dashed curves show the contributions of the various subprocesses. The absolute normalizations are as in Eq. (2), but in order to compare with experimentally measured absolute cross sections one has to invoke additional model assumptions as explained in the text. These $p_T$ shapes are compared with the ones of the $\mu^+\mu^-$ continuum $d^2\sigma/dMdp_T^2$ (dotted curves) in the appropriate mass regions according to the diagrams of Fig. 1. The $\Upsilon$-production data (Ref. 22) are normalized to our predictions at $p_T = 2$ GeV.

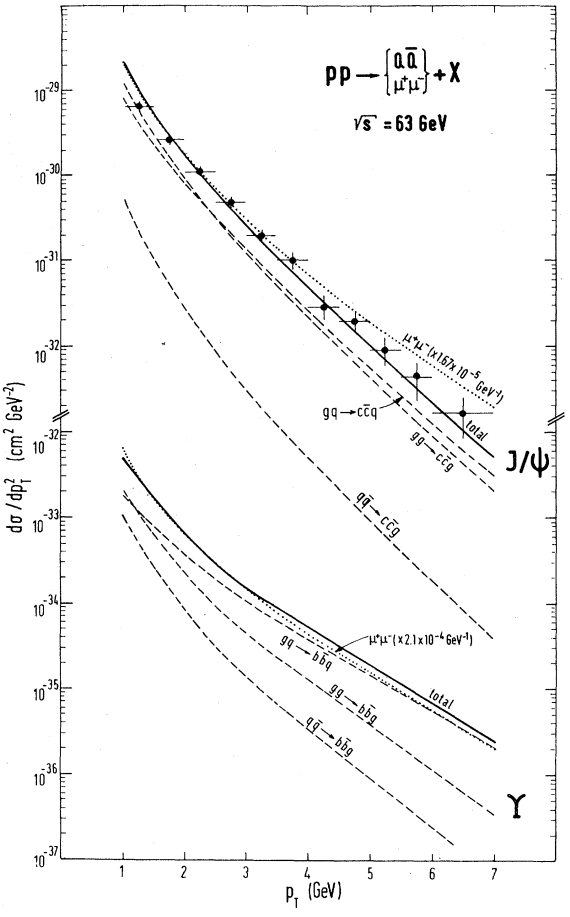


FIG. 4. QCD predictions (solid curves) for the $p_T$ distributions of $J/\psi$ and $\Upsilon$ production at ISR energies. The notation and conventions are as in Fig. 3. The $J/\psi$ production data are taken from Ref. 4.

per) $p_T$ distribution for resonance production than for the $\mu^+\mu^-$ continuum where no $gg$ subprocess exists in leading order. These effects are clearly seen in the $J/\psi$ mass region shown in Figs. 3 and 4 where the predicted $p_T$ spectrum on resonance (solid curve) is significantly steeper than off resonance (dotted curve). The larger the energy becomes, i.e., the larger the steep contribution from the $gg$ process becomes relative to the $gq$ subprocess, the more pronounced this effect will be. At ISR energies, Fig. 4, the transverse momentum distribution of $J/\psi$ production is significantly steeper (solid curve) than for the production of lepton pairs of similar mass (dotted curve). The recent $J/\psi$ measurements at ISR[4] appear to follow our predictions due to the diagrams in Fig. 2 and seem to disagree with the flatter $p_T$ spectrum predicted for the $\mu^+\mu^-$ continuum stemming from the graphs in Fig. 1.

On the other hand at *larger* values of $\sqrt{\tau}$, as is the case in the $\Upsilon$ mass region for example, the $gg$ as well as the $q\bar{q}$ subprocesses will be strongly suppressed because of the decreasing gluon and antiquark wave functions for increasing values of[24] $\sqrt{\tau}$. Thus the $gq \to Q\bar{Q}q$ subprocess will be mainly responsible for the $p_T$ spectrum on resonance which should therefore be similar to the $p_T$ shape off resonance dominated by a similar process $gq \to \mu^+\mu^- q$. Our predictions in Figs. 3 and 4 in the $\Upsilon$ mass region show that this behavior is indeed the case and that the difference in the $p_T$ shape on and off resonance, which is so distinct in the $J/\psi$ region, disappears. Recent ISR data seem to confirm[23] the similarity of the $p_T$ spectra of the $\mu^+\mu^-$ continuum and of $\Upsilon$ production. We therefore expect in general that the average momentum increases for increasing quarkonium mass since the $p_T$ distributions become flatter. Indeed this trend has also been observed experimentally[1,2,4] where, for instance, at ISR energies it has been found[4] that $\langle p_T \rangle_{J/\psi} = (1.2 \pm 0.04)$ GeV and $\langle p_T \rangle_{\Upsilon} = (1.67 \pm 0.18)$ GeV. Additional precision measurements of the $p_T$ spectra on and off resonance in the $J/\psi$ as well as $\Upsilon$ mass region should provide us with a clean test of the two different production mechanisms for heavy-quark bound states and for dimuons and for the different hard scattering processes in Figs. 2 and 1, respectively, responsible for their $p_T$ distributions.

Apart from the absolute normalization, the $p_T$ spectra on and off resonance will always be the same if one adopts the simple approach of Ref. 25 to calculate $d\sigma/dp_T{}^2$ for resonance and $\mu^+\mu^-$ continuum production using the *same* two (massless) subprocesses responsible for transverse dimuon production as shown in Fig. 1. This approach lacks any theoretical basis within the framework of perturbation theory and QCD.

In order to check the sensitivity of our results to the special choice of parton distributions, we have repeated the calculations by turning off the $q^2$ dependence of the parton densities in Eq. (1), i.e., by setting $q^2$ in $f_a^A(x, q^2)$ equal to the input momentum[10] $Q_0{}^2 = 1.8$ GeV$^2$. Since the gluon initiated subprocesses enter dominantly into our predictions we also have repeated the calculations using a broad gluon distribution[26] $xG(x, Q_0{}^2) = 0.8\,(1+9x)(1-x)^4$ which is much harder than the standard one[10] proportional to $(1-x)^5$. In both cases, *all* predicted $p_T$ distributions in Figs. 3 and 4 become flatter by at most 10% but the differences of the $p_T$ shapes on and off resonance remain *unchanged*. On the other hand, the absolute normalization of the cross sections shown will of course significantly change (typically they will increase by a factor 2–10 depending on the reaction and on the kinematical region considered), but these are

TABLE I. Calculated values of $b$ in units of GeV$^{-1}$ according to parametrizing $d\sigma/dp_T^2 \sim \exp(-bp_T)$ in the region $1.5 \leq p_T \leq 3$ GeV. It should be kept in mind that the predicted values of $b$ are *not* constant throughout the whole $p_T$ region and they should be regarded only as an illustration of the *relative* trend of the QCD predictions for $\langle p_T \rangle$ between resonance ($J/\psi, \Upsilon$) and continuum ($\mu^+\mu^-$) production as a function of $\sqrt{s}$.

| | $pp$ | | | | $\bar{p}p$ | | | | $\bar{p}p$ (color singlet) | |
|---|---|---|---|---|---|---|---|---|---|---|
| $\sqrt{s}$ (GeV) | $J/\psi$ | ($\mu^+\mu^-$) | $\Upsilon$ | ($\mu^+\mu^-$) | $J/\psi$ | ($\mu^+\mu^-$) | $\Upsilon$ | ($\mu^+\mu^-$) | $J/\psi$ | $\Upsilon$ |
| 20.6 | 2.7 | (2.7) | 2.6 | (3.0) | 2.6 | (2.4) | 2.7 | (2.7) | 3.1 | 2.8 |
| 27.4 | 2.4 | (2.3) | 1.9 | (2.1) | 2.5 | (2.2) | 2.1 | (2.0) | 3.0 | 2.1 |
| 63 | 2.0 | (1.9) | 1.6 | (1.6) | 2.1 | (1.9) | 1.6 | (1.5) | 2.5 | 1.7 |

sensitive also to other uncertainties as already discussed extensively. Furthermore, we also repeated the calculation using the color-singlet[14] projections of the quarkonium production cross sections in Figs. 2(b) and 2(c); in this case the quarkonium ground states $J/\psi$, $\Upsilon$, etc. are expected to be dominantly produced in association with photons via $p$ waves. In this case the $p_T$ slopes become even steeper on resonance by about 15% than those shown in Figs. 3 and 4, and thus the difference between the $p_T$ slopes of the $J/\psi$ and the corresponding $\mu^+\mu^-$ continuum will be even more pronounced. The absolute normalization for this model would then be smaller by a factor of 5–8.

Although at the present state of the art one cannot calculate reliably $p_T$ moments of heavy quarkonium states, we parametrize our predicted cross sections by $d\sigma/dp_T^2 \sim \exp(-bp_T)$ which is valid in a *limited* $p_T$ region only, say, $1.5 \leq p_T \leq 3$ GeV, from which we might deduce the behavior of $\langle p_T \rangle = 2/b$ for the various processes considered. However, it should be emphasized that this method[4] for calculating the average $p_T$ should be taken with caution since $\langle p_T \rangle$ is sensitive to the small $p_T$ region only where nonperturbative intrinsic $k_T$ smearing effects and $O(\alpha_s^3)$ loop corrections could change even the relative $\langle p_T \rangle$ of the various processes. Nonetheless, we show the results for $b$ in Table I for quarkonium production as compared to the Drell-Yan continuum for $pp$ as well as $\bar{p}p$ scattering. For $pp$ scattering we see that the $p_T$ spectrum of $J/\psi$ is similar to the one of $\mu^+\mu^-$ and both become flatter, i.e., $p_T$ increases, for increasing energy $\sqrt{s}$. In the $\Upsilon$ mass region, however, the $\Upsilon$ has a flatter spectrum than the $\mu^+\mu^-$ continuum for $\sqrt{s} \leq 30$ GeV, whereas at larger (ISR) energies the two spectra become similar. At $\sqrt{s} = 27.4$ GeV we expect $\langle p_T \rangle_{\Upsilon}^{pp}$ to be about 10% larger than $\langle p_T \rangle_{\mu^+\mu^-}^{pp}$, whereas $\langle p_T \rangle_{\Upsilon}^{pp} \simeq \langle p_T \rangle_{\mu^+\mu^-}^{pp}$ for larger (ISR) energies, which is consistent with experiment.[1,4] For $\bar{p}p$ scattering, however, the $b$ values for $J/\psi$ production are always larger than those of the $\mu^+\mu^-$ continuum and therefore we expect $\langle p_T \rangle_{J/\psi}^{\bar{p}p}$ to be smaller than $\langle p_T \rangle_{\mu^+\mu^-}^{\bar{p}p}$ by about 15%, especially for $\sqrt{s} \leq 50$ GeV which is consistent with experiment.[3] On the other hand, in the $\Upsilon$ mass region we expect $\langle p_T \rangle_{\Upsilon}^{\bar{p}p} \simeq \langle p_T \rangle_{\mu^+\mu^-}^{\bar{p}p}$ throughout the whole energy range considered. Table I also shows, as already discussed, that using only color-singlet amplitudes of the gluon-initiated reactions for quarkonium production,[14] one expects a somewhat steeper $p_T$ distribution.

Finally, in Fig. 5 we give predictions for the $p_T$ distributions of $\bar{p}p$ scattering in the $\Upsilon$ mass region at $\sqrt{s} = 540$ GeV. In addition to the flat contribution from the $gq$ subprocess, the steeper $gg$ subprocess contributes a sizable fraction (since $\sqrt{\tau} \simeq 0.02$) and therefore the $p_T$ distribution on resonance is expected to be significantly steeper than the one off resonance ($\mu^+\mu^-$), the latter being dominated by the $gq \to \mu^+\mu^- q$ subprocess. Again, it would be interesting to see whether this distinct difference in the $p_T$ shapes will be confirmed experimentally. Since the $gq \to b\bar{b}q$ and $gg \to b\bar{b}g$ subprocesses dominate throughout the whole $p_T$ region (and not $q\bar{q} \to b\bar{b}g$), the predicted total $p_T$ distribution on resonance is identical in shape *and* absolute normalization for $pp$ collisions, whereas off resonance ($\mu^+\mu^-$) the $p_T$ shape is somewhat flatter than the dotted curve shown in Fig. 5.

## APPENDIX

Here we shall give the explicit analytic expressions for $d\sigma^{ab}$ of the fundamental parton scattering processes which are required in Eqs. (2) and (1) to calculate $d\sigma^{AB}/dp_T^2$ for heavy quarkonium production. To leading order in perturbative QCD, the differential cross section for the production of a massive $Q\bar{Q}$ pair with a hard-gluon emission

$$q(-k_4) + \bar{q}(-k_5) \to \bar{Q}(k_1) + Q(k_2) + g(k_3) \tag{A1}$$

can be written as

$$\frac{d^2\sigma^{q\bar{q}}}{dM dp_T^2} = \frac{\alpha_s^3}{4\pi\hat{s}} \left( \frac{M^2 - 4m_Q^2}{(\hat{s} - M^2)^2 - 4\hat{s}p_T^2} \right)^{1/2} \frac{1}{36} \times \int d\Omega_{TY} W(\{x_{ij}\}, m_Q^2) \tag{A2}$$

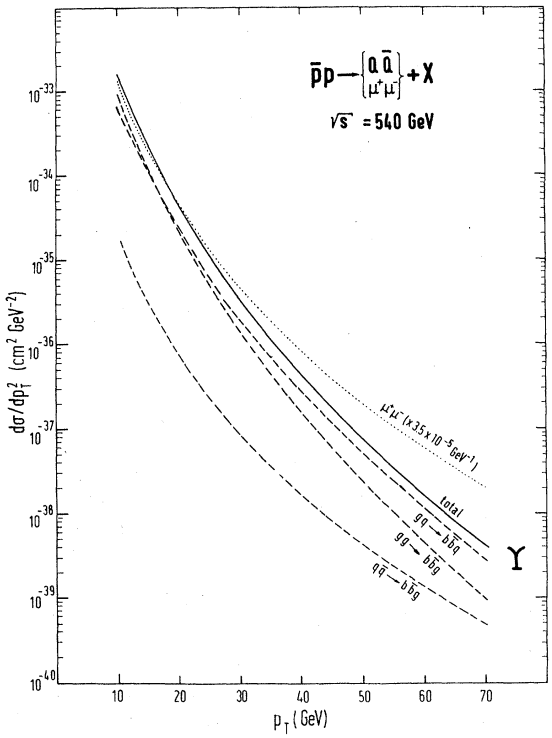


FIG. 5. QCD predictions (solid and dashed curves) for the $p_T$ distribution of Υ production at $\sqrt{s}=540$ GeV. Since the $gq$ and $gg$ subprocesses dominate throughout the whole $p_T$ region, the prediction for the total $p_T$ distribution is the same for $pp$ scattering. For comparison we also show the expected $p_T$ distribution $d^2\sigma/dMdp_T^2$ of the Drell-Yan $\mu^+\mu^-$ continuum (dotted curve); for $pp$ collisions this prediction becomes somewhat flatter at large values for $p_T$ (i.e., a factor of 2 smaller at $p_T$=70 GeV). The conventions are as in Fig. 3.

where $q(-k_4)$ and $\bar{q}(-k_5)$ denote massless quarks with outgoing momenta $k_4$ and $k_5$, $\bar{Q}$ and $Q$ are the final massive quarks with momenta $k_1$ and $k_2$ and mass $m_Q$, and $g$ is the final gluon with momentum $k_3$. The invariant mass of the massive quark pair is denoted by $M$

$$q^2=(k_1+k_2)^2\,, \quad M\equiv(q^2)^{1/2}\,. \tag{A3}$$

The transverse momenta of the quark pair $Q\bar{Q}$ are $\vec{p}_T\equiv\vec{q}_T=(\vec{k}_1+\vec{k}_2)_T$, and $\hat{s}=(k_4+k_5)^2$, and the factor $\frac{1}{36}$ is due to averaging over the initial spin and color states. $d\Omega_{TY}$ denotes the integration over the Treiman-Yang angles (see Fig. 6) defined, in the frame $\vec{q}=0$, via the relations

$$\cos\theta_{TY}=-\left.\frac{\vec{k}_2\cdot\vec{k}_5}{|\vec{k}_2|\,|\vec{k}_5|}\right|_{\vec{q}=0}, \qquad \cos\phi_{TY}=-\left.\frac{(\vec{k}_5\times\vec{k}_2)\cdot(\vec{k}_5\times\vec{k}_3)}{|\vec{k}_5\times\vec{k}_2|\,|\vec{k}_5\times\vec{k}_3|}\right|_{\vec{q}=0}. \tag{A4}$$

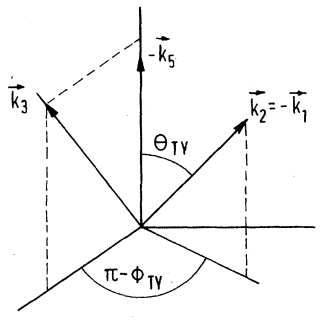


FIG. 6. Definitions of the Treiman-Yang angles.

The function $W(\{x_{ij}\}, m_Q^2)$ in Eq. (A2) is the invariant matrix element squared of the process. It is a rational function of the variables

$$x_{ij}=2k_i\cdot k_j\,, \quad i,j=1,\ldots,5 \tag{A5}$$

and $m_Q^2$. In particular, for the subprocess (A1) we can write

$$W(\{x_{ij}\}, m_Q^2)=\sum_{i,j=1}^{5} C_{ij}\,A_{ij}(\{x_{ij}\}, m_Q^2)\,, \tag{A6}$$

where $C_{ij}$ is a real symmetric matrix of color factors

$$C=\frac{1}{3}\begin{pmatrix} 8 & 1 & 9 & -2 & -7 \\ & 8 & 9 & -7 & -2 \\ & & 18 & -9 & -9 \\ & & & 8 & 1 \\ & & & & 8 \end{pmatrix} \tag{A7}$$

and the matrix elements $A_{ij}(\{x_{ij}\}, m_Q^2)$ are given by the equation

$$A_{ij}=\sum_{\substack{\text{initial, final}\\ \text{spins}}} T_iT_j^*\,, \quad i,j=1,\ldots,5 \tag{A8}$$

where the $T_i$'s denote the Lorentz part of the amplitudes defined by the five Feynman diagrams in Fig. 7.

It is convenient to introduce symmetric matrices $N_{ij}$ and $D_{ij}$,

$$A_{ij}=-16\,\frac{N_{ij}}{D_{ij}}\,, \tag{A9}$$

which are homogeneous functions of the $x_{ij}$'s and of $m_Q^2$. In terms of the variables

$$s_{ij}=(k_i+k_j)^2=x_{ij}+m_i^2+m_j^2$$

the denominator matrix $D_{ij}$ in Eq. (A9) has the following form

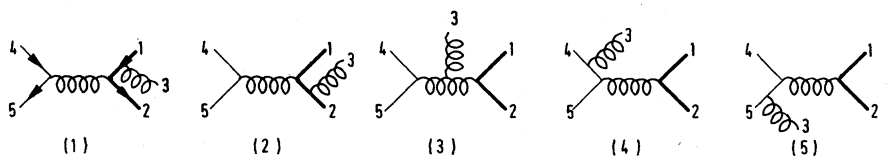


FIG. 7. Feynman diagrams for the reaction $q(-k_4)+\bar{q}(-k_5)\to\bar{Q}(k_1)+Q(k_2)+g(k_3)$ where the heavy-quark $Q$ states are denoted by heavy lines.

$$D=\begin{pmatrix} x_{31}^2x_{54}^2, & 2x_{23}x_{31}x_{54}^2, & 4s_{12}x_{31}x_{54}^2, & 2s_{12}x_{31}x_{43}x_{54}, & 2s_{12}x_{31}x_{53}x_{54} \\ & x_{23}^2x_{54}^2, & 4s_{12}x_{23}x_{54}^2, & 2s_{12}x_{23}x_{43}x_{54}, & 2s_{12}x_{23}x_{53}x_{54} \\ & & 4s_{12}^2x_{54}^2, & 4s_{12}^2x_{43}x_{54}, & 4s_{12}^2x_{53}x_{54} \\ & & & s_{12}^2x_{43}^2, & 2s_{12}^2x_{43}x_{53} \\ & & & & s_{12}^2x_{53}^2 \end{pmatrix} \tag{A10}$$

and for the matrix elements $N_{ij}$ we find

$$\begin{aligned}
N_{11}&=x_{31}(-x_{42}x_{53}-x_{43}x_{52}+2m_Q^2x_{54})+2m_Q^2(x_{41}x_{52}+x_{42}x_{51}+x_{42}x_{53}+x_{43}x_{52}+2m_Q^2x_{54}),\\
N_{12}&=x_{12}[x_{41}(2x_{52}+x_{53})+x_{42}(2x_{51}+x_{53})+x_{43}(x_{51}+x_{52})+4m_Q^2x_{54}]\\
&\quad+x_{23}[x_{41}(-2x_{51}+x_{52})+x_{42}x_{51}+2m_Q^2x_{54}]\\
&\quad+x_{31}[x_{41}x_{52}+x_{42}(x_{51}-2x_{52})+2m_Q^2x_{54}]-4m_Q^2x_{43}x_{53},\\
N_{13}&=x_{12}[-2x_{31}x_{54}+x_{41}(4x_{52}+3x_{53})+x_{42}(4x_{51}+3x_{53})+x_{43}(3x_{51}+3x_{52}+2x_{53})+8m_Q^2x_{54}]\\
&\quad+x_{23}[x_{41}(-6x_{51}+x_{52}-x_{53})+(x_{42}-x_{43})x_{51}+4m_Q^2x_{54}]\\
&\quad+x_{31}[x_{41}x_{52}+x_{42}(x_{51}-2x_{52}-3x_{53})-3x_{43}x_{52}]\\
&\quad+2m_Q^2[x_{41}(2x_{51}+4x_{52}+3x_{53})+x_{42}(4x_{51}-2x_{52}+5x_{53})+x_{43}(3x_{51}+5x_{52})+8m_Q^2x_{54}],\\
N_{14}&=x_{51}(-x_{12}x_{43}+x_{23}x_{41}+x_{42}x_{43})+x_{31}[2x_{41}x_{52}+x_{42}(x_{51}-x_{54})+2x_{43}x_{52}+2m_Q^2x_{54}]\\
&\quad+x_{41}[2(x_{41}+x_{43})x_{52}+x_{42}(2x_{51}+x_{53})+2m_Q^2(x_{53}+2x_{54})]+2m_Q^2x_{43}(x_{53}+x_{54}-x_{51}-x_{52}),\\
N_{15}&=N_{14}(4\leftrightarrow5),\quad N_{22}=N_{11}(1\leftrightarrow2),\quad N_{23}=N_{13}(1\leftrightarrow2),\quad N_{24}=N_{14}(1\leftrightarrow2),\quad N_{25}=N_{24}(4\leftrightarrow5),\\
N_{33}&=x_{12}[2x_{54}(x_{12}-x_{23}-x_{31})+x_{41}(-2x_{51}+6x_{52}+5x_{53})+x_{42}(-2x_{52}+6x_{51}+5x_{53})\\
&\quad+x_{43}(5x_{51}+5x_{52}+4x_{53})+28m_Q^2x_{54}]\\
&\quad+x_{23}[-2x_{31}x_{54}+x_{41}(-6x_{51}+x_{52}-3x_{53})+(x_{42}-3x_{43})x_{51}]\\
&\quad+x_{31}[x_{41}x_{52}+x_{42}(x_{51}-6x_{52}-3x_{53})-3x_{43}x_{52}]\\
&\quad+2m_Q^2[x_{41}(-4x_{51}+4x_{52}+7x_{53})+x_{42}(4x_{51}-4x_{52}+7x_{53})+x_{43}(7x_{51}+7x_{52}+2x_{53})+24m_Q^2x_{54}],\\
N_{34}&=x_{12}[x_{54}(x_{23}+x_{31}+x_{42}+x_{41})-2x_{43}(x_{51}+x_{52})]\\
&\quad+x_{23}[2x_{31}x_{54}+x_{41}(x_{52}-x_{53}-x_{54})+3x_{51}(x_{42}+x_{43})+8m_Q^2x_{54}]\\
&\quad+x_{31}[x_{42}(x_{51}-x_{53}-x_{54})+3x_{52}(x_{41}+x_{43})+8m_Q^2x_{54}]\\
&\quad+x_{41}[3(x_{41}+x_{43})x_{52}+x_{42}(x_{51}+x_{52}+2x_{53})+2m_Q^2(x_{53}+5x_{54})]\\
&\quad+x_{42}[3(x_{42}+x_{43})x_{51}+2m_Q^2(x_{53}+5x_{54})]+2m_Q^2x_{43}(2x_{53}+2x_{54}-5x_{51}-5x_{52}),\\
N_{44}&=x_{43}(-x_{23}x_{51}-x_{31}x_{52}-2m_Q^2x_{53}),\\
N_{45}&=x_{54}[x_{23}(x_{41}+x_{51})+x_{31}(x_{42}+x_{52})+4m_Q^2(x_{53}+x_{54}+x_{43})]\\
&\quad+x_{41}[x_{52}(x_{43}+2x_{54})+x_{53}(x_{52}-2x_{42})]+x_{51}[-2x_{43}x_{52}+x_{42}(x_{53}+2x_{54}+x_{43})],\\
N_{35}&=N_{34}(4\leftrightarrow5),\quad N_{55}=N_{44}(4\leftrightarrow5).
\end{aligned} \tag{A11}$$

The cross section for the subprocess

$$q(-p_4)+g(-p_5)\to\bar{Q}(p_1)+Q(p_2)+q(p_3) \qquad \text{(A12)}$$

can be easily obtained from Eq. (A2) by the use of crossing symmetry. Interchanging the antiquark line with the gluon line, modifying the spin and color average factor, and introducing a negative overall sign, we get

$$\frac{d^2\sigma^{gq}}{dM\,dp_T{}^2}=-\frac{\alpha_s{}^3}{4\pi\bar{s}}\left(\frac{M^2-4m_Q{}^2}{(\bar{s}-M^2)^2-4\bar{s}p_T{}^2}\right)^{1/2}\frac{1}{96}$$

$$\times\int d\tilde{\Omega}_{\mathrm{TY}}\,W(\{x_{ij}\},m_Q{}^2)\,, \qquad \text{(A13)}$$

where $\bar{s}=(p_4+p_5)^2$ and the Treiman-Yang angles are now defined in terms of $\vec{p}_i$, similarly to Eq. (A4), by

$$\cos\tilde{\theta}_{\mathrm{TY}}=-\left.\frac{\vec{p}_2\cdot\vec{p}_5}{|\vec{p}_2|\,|\vec{p}_5|}\right|_{\vec{p}_1=-\vec{p}_2},$$

$$\cos\tilde{\phi}_{\mathrm{TY}}=-\left.\frac{(\vec{p}_5\times\vec{p}_3)\cdot(\vec{p}_5\times\vec{p}_2)}{|\vec{p}_5\times\vec{p}_3|\,|\vec{p}_5\times\vec{p}_2|}\right|_{\vec{p}_1=-\vec{p}_2}.$$

The invariant matrix element squared $W(\{x_{ij}\},m_Q{}^2)$ is the same function as given by Eqs. (A6)–(A11). The physical region of the variables $x_{ij}$, however, is different: They are defined by Eq. (A5) in terms of the vectors $k_i$'s,

$$k_i=p_i \text{ if } i=1,2,4, \text{ and } k_3=p_5,\ k_5=p_3\,. \qquad \text{(A14)}$$

The algebraic formula obtained for the invariant function $\bar{W}$ for the subprocess

$$g(-l_4)+g(-l_5)\to\bar{Q}(l_1)+Q(l_2)+g(l_3) \qquad \text{(A15)}$$

is exceedingly longer than the expressions given by Eqs. (A6)–(A11). In this case we have 16 Feynman diagrams, where 3- and 4-gluon vertices occur more frequently. Furthermore, there are complications due to the summation over the gluon helicities since either a helicity projector has to be used,

$$\sum_{\text{pol}}\epsilon_\mu\epsilon_\nu=-g_{\mu\nu}+\frac{k_\mu n_\nu+k_\nu n_\mu}{k\cdot n}-\frac{k_\mu k_\nu}{(k\cdot n)^2}\,, \qquad \text{(A16)}$$

where $n_\mu$ is an arbitrary timelike unit vector ($n^2=+1$), or one can replace the sum $\sum\epsilon_\mu\epsilon_\nu$ with $-g_{\mu\nu}$ but then the contributions of ghost diagrams have to be subtracted in order to eliminate the unphysical longitudinal gluon polarization component. In the algebraic calculation with REDUCE it was more convenient to apply the second method. We also calculated the function $\bar{W}(\{x_{ij}\},m_Q{}^2)$ at several phase-space points with the help of an entirely numerical method, in which the helicity projector (A16) has been used. The virtue of the algebraic expression is obvious: The calculation of the value of the function $\bar{W}$ at a given point with the help of the numerical program was slower by a factor of about 200.

Finally we mention that if we allow production of the final quark pair only in a color-singlet state[14] then we should only change the color matrix in Eq. (A7) to

$$C^{\text{singlet}}=\frac{1}{3}\begin{bmatrix}1&-1&0&0&0\\-1&1&0&0&0\\0&0&0&0&0\\0&0&0&0&0\\0&0&0&0&0\end{bmatrix}. \qquad \text{(A17)}$$

*Permanent address: Eötvös University, Budapest, Hungary.

[1]D. M. Kaplan *et al.*, Phys. Rev. Lett. 40, 435 (1978).
[2]J. G. Branson *et al.*, Phys. Rev. Lett. 38, 1331 (1977).
[3]K. J. Anderson *et al.*, University of Chicago Report No. EFI 78-38, paper submitted to the 19th International Conference on High Energy Physics, Tokyo, 1978 (unpublished); Phys. Rev. Lett. 42, 944 (1979).
[4]C. Kourkoumelis *et al.*, Brookhaven Report No. BNL-25075, paper submitted to the 19th International Conference on High Energy Physics, Tokyo, 1978 (unpublished).
[5]H. D. Politzer, Nucl. Phys. B129, 301 (1977); A. V. Radyushkin, Phys. Lett. 69B, 245 (1977).
[6]H. Fritzsch and P. Minkowski, Phys. Lett. 73B, 80 (1978); G. Altarelli, G. Parisi, and R. Petronzio, *ibid.* 76B, 351 (1978).
[7]K. Kajantie and R. Raitio, Nucl. Phys. B139, 72 (1978).
[8]For a complete list of references we refer the reader to the review of F. Halzen, in *Proceedings of the 19th International Conference on High Energy Physics, Tokyo*, 1978; edited by S. Hamma, M. Kawaguchi, H. Miyazawa (Phys. Soc. of Japan, Tokyo, 1979), p. 214; Wisconsin Report No.COO-881-53(unpublished).
[9]F. Halzen and D. M. Scott, Phys. Rev. Lett. 40, 1117 (1978); Phys. Rev. D 18, 3378 (1978).
[10]J. F. Owens and E. Reya, Phys. Rev. D 17, 3003 (1978).
[11]M. Glück and E. Reya, Nucl. Phys. B145, 24 (1978).
[12]Yu. L. Dokshitzer, D. I. D'yakonov, and S. I. Troyan, Phys. Lett. 78B, 290 (1978); 79B, 269 (1978).
[13]G. Parisi and R. Petronzio, Nucl. Phys. B154, 427 (1979).
[14]M. B. Einhorn and S. D. Ellis, Phys. Rev. D 12, 2007 (1975).
[15]H. Fritzsch, Phys. Lett. 67B, 217 (1977).
[16]M. Glück, J. F. Owens, and E. Reya, Phys. Rev. D 17, 2324 (1978).
[17]L. M. Jones and H. W. Wyld, Phys. Rev. D 17, 2332 (1978).
[18]C. E. Carlson and R. Suaya, Phys. Rev. D 18, 760 (1978); Phys. Lett. 81B, 329 (1979).
[19]M. Glück and E. Reya, Phys. Lett. 79B, 453 (1978).
[20]Z. Kunzst and E. Pietarinen, Z. Phys. C (to be pub-

lished).
[21]A. C. Hearn, REDUCE 2. University of Utah report, 1965 (unpublished).
[22]K. Ueno *et al.*, Phys. Rev. Lett. 42, 486 (1979).
[23]U. Becker, Nordic Particle Physics Meeting, NORDITA, Copenhagen, 1979 (unpublished).
[24]The dominant contribution to the integral in Eq. (1) comes from the region where $x_a \simeq x_b \simeq \sqrt{\tau}$.
[25]F. Halzen, J. P. Leveille, and D. M. Scott, University of Wisconsin—Madison, Report No. COO-881-95, 1979 (unpublished).
[26]R. P. Feynman, R. D. Field, and G. C. Fox, Phys. Rev. D 18, 3320 (1978).